



Molecular structure and reactivity of Vitamin B6/salicylaldehyde containing model enzymes
by Andrew Gilchrist Sykes

A thesis submitted in partial fulfillment of the requirements for the degree of Master of Science in
Chemistry

Montana State University

© Copyright by Andrew Gilchrist Sykes (1984)

Abstract:

Deuterium exchange of the two glycine protons in sodium bis(pyridoxylidene-glycinato)cobaltate(III) is examined. Second order rate constants for exchange in a carbonate/deuterated bicarbonate buffer in D₂O are determined, and activation parameters are calculated accordingly. Glycine protons exhibit differing reactivities, the faster proton exchanged roughly ten times the rate of the slow proton over a thirty degree temperature range. The difference in reactivities is attributed to greater ζ - π overlap of the fast proton in the transition state, and both NMR of the complex in solution and crystallographic evidence support the different orientations of glycine protons to the neighboring pi system. Activation parameters for the fast proton are $\Delta H^\ddagger = 9.9 \pm 2$ kcal/mole and $\Delta S^\ddagger = -28 \pm 7$ e.u., and $\Delta H^\ddagger = 14.5 \pm 1$ kcal/mole and $\Delta S^\ddagger = -17 \pm 4$ e.u. for the slow proton. These energies differ in numerical magnitude from activation parameters done in a previous study.

MOLECULAR STRUCTURE AND REACTIVITY
OF VITAMIN B₆/SALICYLALDEHYDE
CONTAINING MODEL ENZYMES

by

Andrew Gilchrist Sykes

A thesis submitted in partial fulfillment
of the requirements for the degree

of

Master of Science

in

Chemistry

MONTANA STATE UNIVERSITY
Bozeman, Montana

October 1984

MAN 110
N378
S4 44
COP 2

APPROVAL

of this thesis submitted by

Andrew Gilchrist Sykes

This thesis has been read by each member of the thesis committee and has been found to be satisfactory regarding content, English usage, format, citations, bibliographic style, and consistency, and is ready for submission to the College of Graduate Studies.

10/8/84
Date

Edwin H. Abbott
Chairperson, Graduate Committee

Approved for the Major Department

10/8/84
Date

Edwin H. Abbott
Head, Major Department

Approved for the College of Graduate Studies

10-9-84
Date

Michael P. Malone
Graduate Dean

STATEMENT OF PERMISSION TO USE

In presenting this thesis in partial fulfillment of the requirements for a master's degree at Montana State University, I agree that the Library shall make it available to borrowers under rules of the Library. Brief quotations from this thesis are allowable without special permission, provided that accurate acknowledgment of source is made.

Permission for extensive quotation from or reproduction of this thesis may be granted by my major professor, or in his absence, by the Director of Libraries when, in the opinion of either, the proposed use of the material is for scholarly purposes. Any copying or use of the material in this thesis for financial gain shall not be allowed without my written permission.

Signature



Date

10/8/84

To my grandparents with love,

Edith Reed VanHorn
and
Bert Allison VanHorn

Dorthy O'Neil Sykes
and
Edwin Gilchrist Sykes

ACKNOWLEDGMENTS

I would like to take this opportunity to thank the following people for their support and invaluable assistance without which this project would have not been possible.

To Ray Larson, I extend my gratitude for his genius in crystallography. I also wish to thank Jim Fischer of Western New Mexico College for his kinetic and synthetic knowhow and for getting the ball rolling in the first place. My colleagues in research, Mark Anderson, Scott Busse, and Eric Peterson deserve great praise as well for an enjoyable and worthwhile two years.

I would especially like to thank Dr. Edwin H. Abbott for his never ending positiveness and direction, combined with good philosophy and patience in guiding me through this project.

Finally, I express my deep gratitude for my parents, Richard and Virginia Sykes, for their continual love and encouragement.

TABLE OF CONTENTS

| | Page |
|-------------------------------|------|
| LIST OF TABLES..... | vii |
| LIST OF FIGURES..... | viii |
| ABSTRACT..... | x |
| INTRODUCTION..... | 1 |
| STATEMENT OF OBJECTIVES..... | 12 |
| KINETIC RESULTS..... | 13 |
| CRYSTALLOGRAPHIC RESULTS..... | 25 |
| DISCUSSION..... | 35 |
| EXPERIMENTAL..... | 47 |
| NOTES AND REFERENCES..... | 54 |

LIST OF TABLES

| | Page |
|---|------|
| Table 1. First order rate data, A proton, 13°C..... | 20 |
| Table 2. First order rate data, A proton, 20°C..... | 20 |
| Table 3. First order rate data, A proton, 32°C..... | 21 |
| Table 4. First order rate data, A proton, 42°C..... | 21 |
| Table 5. First order rate data, B proton, 3°C..... | 22 |
| Table 6. First order rate data, B proton, 13°C..... | 22 |
| Table 7. First order rate data, B proton, 21°C..... | 23 |
| Table 8. First order rate data, B proton, 33°C..... | 23 |
| Table 9. Second order rate data..... | 24 |
| Table 10. Bond angles (°)..... | 31 |
| Table 11. Angles in the coordination polyhedron around Co | 31 |
| Table 12. Bond lengths (Å)..... | 32 |
| Table 13. Anisotropic thermal parameters..... | 32 |
| Table 14. Atomic coordinates and isotropic thermal parameters..... | 33 |
| Table 15. H-atom coordinates and isotropic thermal parameters..... | 34 |
| Table 16. Hydrogen bonds..... | 34 |
| Table 17. Crystallographic data..... | 53 |

LIST OF FIGURES

| | Page |
|---|------|
| Figure 1. Non-enzymatic pyridoxal-Schiff base model..... | 2 |
| Figure 2. The Snell Mechanism..... | 3 |
| Figure 3. 3 β -acetoxycholestan-7-one..... | 6 |
| Figure 4. Favored paths of enolization and protonization of testosterone..... | 7 |
| Figure 5. (1) Co(III) pyridoxylidene glycine; (2) substituted Co(III) salicylidene glycine..... | 9 |
| Figure 6. ^1H NMR decay of the glycine AB pattern showing deuterium exchange of the fast B proton..... | 14 |
| Figure 7. ^1H NMR decay of the glycine AB pattern showing deuterium exchange of the slow A proton..... | 15 |
| Figure 8. Typical first order rate plot of integrated NMR peak areas vs. time..... | 16 |
| Figure 9. Second order kinetic plot of the slow A proton at 32°C..... | 17 |
| Figure 10. Temperature dependence for the second order rate constants for exchange of the glycine protons of Co(III) pyridoxylidene glycine. Both protons have correlations greater than 0.990..... | 19 |
| Figure 11. Structure of the complex anion with averaged bond lengths and angles..... | 25 |
| Figure 12. Projections of ligands on CoO(1)O(2)N(1) and CoO(1')O(2')N(1') planes..... | 27 |
| Figure 13. Crystal packing of TMA{Co(PGly) $_2$ } viewed along the b axis. TMA cations are shaded dark, and water molecules are labeled and connected by dashed lines..... | 30 |
| Figure 14. Co(III) pyridoxylidene glycine illustrating axial and equatorial positions of the glycine protons..... | 36 |

LIST OF FIGURES-Continued

| | Page |
|---|------|
| Figure 15. Similar puckering of 5-membered metalocycle of Co(III) 3-methyl salicylidene threonine.... | 36 |
| Figure 16. Distortion of one ligand of Co(III) salicylidene glycine while the other remains virtually planar..... | 38 |
| Figure 17. Distorted Δ isomer of Co(III) pyridoxylidene valine..... | 38 |
| Figure 18. Allylic fragment of Co(PGly) ₂ demonstrating the dihedral angle dependence..... | 40 |
| Figure 19. AB pattern of the glycine protons along with long distant, allylic coupling by the azomethine proton. Other peaks are the 5-CH ₂ group and a suppressed solvent peak..... | 42 |
| Figure 20. ¹ H NMR spectrum of Co(III) pyridoxylidene glycine..... | 49 |

ABSTRACT

Deuterium exchange of the two glycine protons in sodium bis(pyridoxylidene-glycinato)cobaltate(III) is examined. Second order rate constants for exchange in a carbonate/deuterated bicarbonate buffer in D_2O are determined, and activation parameters are calculated accordingly. Glycine protons exhibit differing reactivities, the faster proton exchanged roughly ten times the rate of the slow proton over a thirty degree temperature range. The difference in reactivities is attributed to greater σ - π overlap of the fast proton in the transition state, and both NMR of the complex in solution and crystallographic evidence support the different orientations of glycine protons to the neighboring pi system. Activation parameters for the fast proton are $\Delta H^\ddagger = 9.9 \pm 2$ kcal/mole and $\Delta S^\ddagger = -28 \pm 7$ e.u., and $\Delta H^\ddagger = 14.5 \pm 1$ kcal/mole and $\Delta S^\ddagger = -17 \pm 4$ e.u. for the slow proton. These energies differ in numerical magnitude from activation parameters done in a previous study.

INTRODUCTION

Involved in the metabolism of amino acids is the cleavage of some chemical grouping to the α -carbon. Cleavage of the C_{α} -COOH or C_{α} -H bond is thermodynamically most unfavourable since pKa values of an unmodified amino acid alpha carbon lie in excess of 30, rendering ΔG° values approximately equal to 38 kcal/mole or greater. Only through some persuasive form of catalysis can the metabolism of amino acids be realized.

The original discovery leading to the interest in pyridoxal dependent biological reactions, the key to the catalysis puzzle, was made in 1934 by Paul Gyorgy of Western Reserve University.¹ This nutritional factor, which Gyorgy called vitamin B₆, was subsequently identified as pyridoxine, one of a number of closely related compounds in the B₆ grouping, pyridoxal among them.

Pyridoxal's utility as a catalytic agent became apparent when it was recognized formation of a Schiff base between the cofactor and an amino acid greatly affected rates of alpha carbon cleavages. In 1952, Metzler and Snell expanded the field even further when they published a pyridoxal-dependent, non-enzymatic

transamination in the presence of metal ions.² Numerous enzymatic reactions have now been reproduced using the metal-amino acid-pyridoxal model system proposed by Snell, all having the basic features shown in Figure 1.

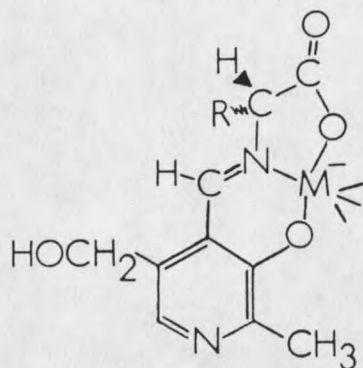


Figure 1. Non-enzymatic pyridoxal-Schiff base model.

A number of these non-enzymatic reactions, paralleling the enzymatic, biological reactions, are condensed in Figure 2, demonstrating the enormous versatility of the model system. Common in all pathways, however, is the initial loss of an electropositive substituent from the alpha carbon. Loss of the substituent and consequent formation of negative charge on the alpha carbon is relieved through two structural features of the model system. One, the conjugated pi system transfers electrons through the molecule and coordinates a proton on the pyridine nitrogen. Two, the metal ion itself is electronegative, reducing electronic

THE SNELL MECHANISM*

* Metzler, Ikawa, & Snell, JACS, **76**, 648(1954).

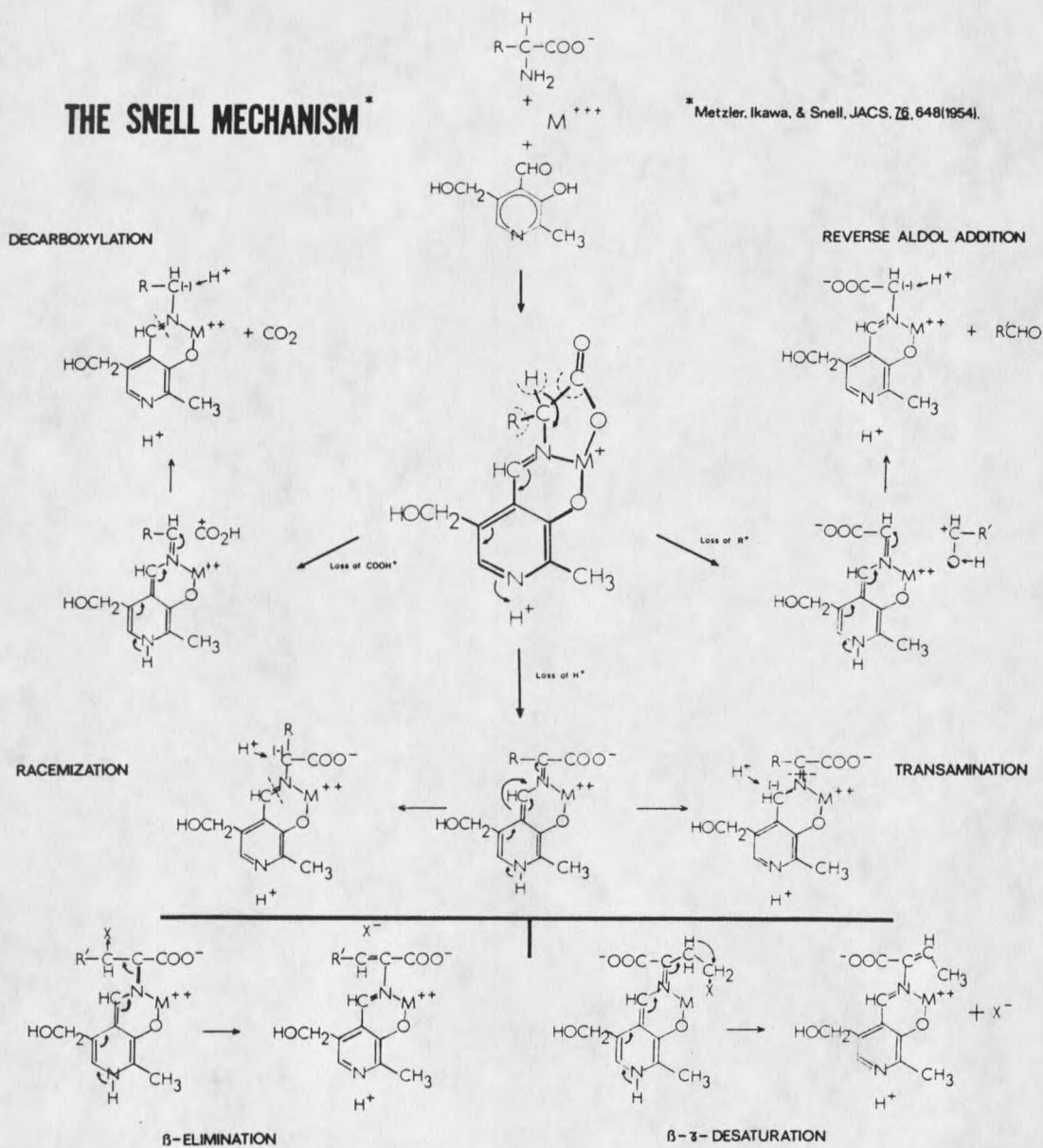


Figure 2. The Snell Mechanism.³

charge on the alpha carbon. Both these effects have a catalytic value, lowering the carbanionic character of the alpha carbon and increasing rates of reactions, reactions unlikely without such assistance. Furthermore, the metal ion locks the molecule into a particular constrained conformation as will be discussed further on.

Though metal ions in model systems are not obligatory for amino acid transformations (some do proceed without metal ions present), their presence has generally been found to greatly enhance reaction rates and product formation. In pyridoxal-dependent enzymes themselves, however, it is unlikely metal ions play an active role. Certainly it is the prosthetic groups of pyridoxal combined that leads to the cofactors utility. The pyridinium nitrogen, the 5-hydroxy or phosphate group, plus the carboxylic group of the amino acid all must fit or bind into the particular pattern of the enzyme in such a way as to lower the pKa value of the relevant carbon acid-whether or not in the presence of metals.

Even despite limiting evidence of metalloenzymes, the remarkable work commenced by Snell and his associates in the early 50's has led to a group of metal complexes successful in reproducing the reactions of metal-free or metal-containing biological molecules. The scope

delimiting the types and methods of non-enzymatic model reactions is now rather complete. What remains to be done is significant research activity in coordination chemistry and catalysis, and even more remains to be understood about the structural and electronic features of the complexes themselves. To provide a clearer understanding of reactivities, precise structural determinations need to be made along with further detailed kinetic studies of the various transformations as well. Helping understand the factors controlling reactivities of substituents at amino alpha carbons in complexes such as in Figure 1, then, is the general intent of this thesis.

The hypothesis of Snell concerning the mechanism of amino acid transformations emphasizes the function of the cofactor and metal ion in weakening the sigma bonds around the alpha carbon, but it does not address the question about which bond is cleaved most easily. For example, why the preferential loss of one alpha carbon substituent over another? In the late sixties, H.C. Dunathan attributed the stereochemical relationship of the sigma bond to the adjacent pi system as being responsible for determining reaction specificity.⁴ Since loss of a group from the amino acid alpha carbon results in carbanion formation and the extension of the pyridoxal

imine system, an increase in delocalization energy occurs. If this gain in delocalization energy is to aid in bond breaking, a geometry placing the bond to be broken perpendicular to the pyridoxal imine system (coplanar with the pi system) is most highly favoured. Thus, transition states where sigma bond to pi system interactions are as coplanar as possible will enhance reactivities. It is expected bond breakage assisted by delocalization energy will have lower enthalpies of activation than sigma bonded substituents bonded more perpendicular to the pi system.

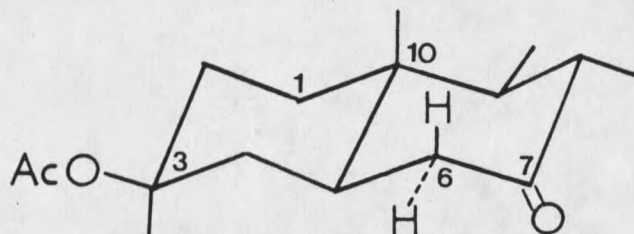


Figure 3. 3β -acetoxycholestan-7-one.

Early work done by Corey on the stereochemistry of enolization of 3β -acetoxycholestan-7-one (Figure 3) showed clear preference for bromination to occur axially at the 6-methylene carbon.⁵ Opposing this effect is the classical steric argument, more 1,3-interactions, which directs a substituent as large as bromine towards the less crowded equatorial position. Obviously, the axial

product is formed kinetically rather than for thermodynamic reasons, and it is thought in the transition state, since the enolization-ketonization process is stabilized by bonding between alpha and carbonyl carbons involving $\sigma-\pi$ delocalization, there should be a demonstrated preference for loss or gain of an axial alpha substituent. Subsequently an axial hydrogen is lost in enol formation and return of bromine occurs likewise in the more hindered axial position. This is the same phenomenon as described by Dunathan above.

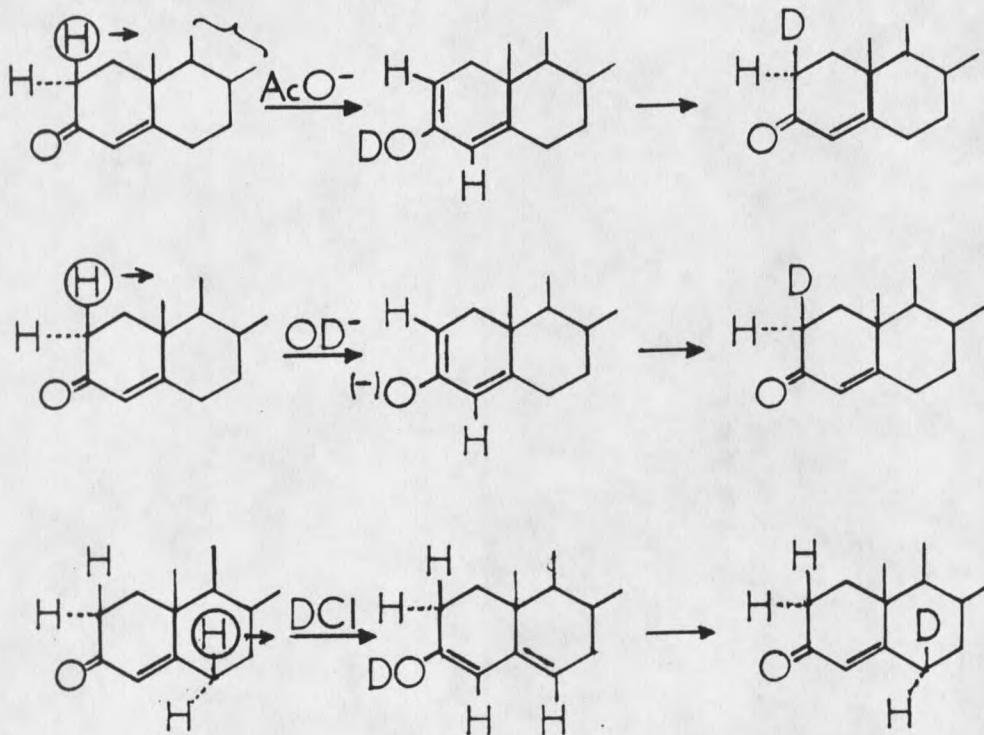


Figure 4. Favored paths of enolization and protonation of testosterone.

Malhotra and Ringold studied the kinetically controlled enolization of testosterone (Figure 4).⁶ Both NaOD and CH₃COOD in D₂O catalyzed deuterium exchange at the 2-position immediately adjacent to the carbonyl group, and exchange, in both cases, occurred axial as well. Deuterium chloride catalysis resulted in the preferential loss and exchange of the C-6 proton. This change in specificity is attributed to base strength. Using strong base, CH₃COO⁻ or OD⁻, the determining factor in the transition state is the acidity of the methylenic protons. C-2 protons next to the carbonyl being are more acidic than the C-6 protons, and at the C-2 carbon, the axial proton is more labile than the equatorial proton for reasons put forth above. With DCl catalysis however, since D₂O is the strongest base present, considerable C-H bond stretching in the transition state will lead to a greater resemblance to enol. Acidity (C-2 vs. C-6) will assume little relative importance, and stability now hinges on the respective enols themselves. It should be noted though that even with DCl catalysis, the more acidic axial C-6 proton was lost and preferentially replaced with retention of configuration.

Recent studies have focused on the kinetics of deuterium exchange between glycine protons of the alpha carbon in the following model systems (Figure 5).

